Conductance transition and interwire ordering of Pb nanowires on Si(557)

Harumo Morikawa and Keun Su Kim

Center for Atomic Wires and Layers, Pohang University of Science and Technology, Pohang 790-784, Korea

Yusuke Kitaoka, Toru Hirahara, and Shuji Hasegawa

Department of Physics, School of Science, The University of Tokyo, 7-3-1 Hongo, Bunkyo-ku, Tokyo 113-0033, Japan

Han Woong Yeom[*]

Center for Atomic Wires and Layers and Department of Physics, Pohang University of Science and Technology, Pohang 790-784, Korea

A Pb-nanowire array on a stepped Si surface, Si(557)$\alpha \times 2$-Pb, is investigated by surface-state conductivity measurements, scanning-tunneling microscopy (STM), and angle-resolved photoelectron spectroscopy (ARPES). No clear indication was found for the abrupt phase transition at 78 K, which was reported to exhibit a switching from a two-dimensional semiconducting conductivity to an one-dimensional metallic behavior and to accompany an intrawire ordering together with a change in the interwire periodicity (so-called "refaceting"). In contrast, a significant reduction in the surface conductivity is found at around 140 K. This transition is accompanied by a subtle out-of-phase interwire ordering of the protrusions along wires in STM images. However, ARPES finds no sign of a significant electronic structure change. While we cannot rule out the possibility of a phase transition at 78 K within a very limited coverage range, this metal-insulator-type transition is found to prevail for most of Pb coverages with a good $\alpha \times 2$ ordering. The conductivity below 80 K can be described by the weak localization in two dimensions probably due to the interwire ordering but the abrupt transition at 140 K itself cannot easily be explained at present.

I. INTRODUCTION

Intriguing properties of low-dimensional metals have attracted substantial interest from both theoretical and experimental points of view. Some of them exhibit, at low temperature, metal-insulator transitions (MITs) and others anisotropic superconductivity.[1–3] While these properties have been intensively studied with bulk low-dimensional crystals, growing efforts were recently made for low-dimensional metals on solid surfaces. Atomically well-defined metallic wires and layers were fabricated by choosing proper substrates and adsorbates.[4] One of the advantages of surface systems is that they can be directly probed by various powerful surface-sensitive experimental techniques, such as angle-resolved photoelectron spectroscopy (ARPES) and scanning-tunneling microscopy (STM). Moreover, a recently developed method, the micro-four-point-probe (μ4PP) technique, has enabled surface-sensitive electron-transport measurements.[5] These techniques have been successfully utilized to investigate interesting phase transitions and intriguing electronic properties of low-dimensional metals on surfaces.[5–15]

As prototype one-dimensional (1D) metals on solid surfaces, atomic wire arrays on silicon surfaces, such as Si(111)4 $\times$ 1-In and Si(553)-Au, are characterized by well-ordered atomic chain structures and strongly anisotropic band structures.[7,16] Their well-nested Fermi surfaces (FSs) lead to Peierls-type MITs upon cooling with periodic lattice distortions.[6–9] However, the Pb-nanowire (nanostripe) array found recently on Si(557), so-called Si(557)$\alpha \times 2$-Pb ($\alpha \times 2$-Pb hereafter), exhibits distinct behavior. This structure forms (223) facets on Si(557) and has an interwire spacing of 15.4 Å with a $2a_0$-period structure along the wires [a_0

$= 3.84$ Å the lattice constant of Si(111)].[17,18] In sharp contrast to the strongly anisotropic atomic structure with wires separated by Si-bilayer steps, the electronic structure of the Pb-nanowire array could be explained with two-dimensional (2D) bands modulated moderately by a weak step potential.[19,20] Moreover, the previous conductance measurement with a conventional *macroscopic* 4PP showed a peculiar conductance transition from a 2D semiconducting behavior to a 1D metal at 78 K.[21,22] This transition was suggested to originate from a very complicated structural change at low temperature; the freezing of dynamic structural fluctuations in the intrawire modulation[23] to form a long-period ($10a_0$) superstructure along the wires and also, the freezing of the dynamically fluctuating interwire spacing (so-called "dynamic refacetting").[24] The previous low-energy electron diffraction (LEED), STM, and ARPES measurements at low temperature suggested the formation of a $10a_0$ modulation. However, the interconnection of these experimental results is hardly demystified. For example, the semiconducting behavior in conductance for the high-temperature phase is not straightforward from the 2D metallic band structure in ARPES. It is also not clear at all why the refacetting yields a $10a_0$ modulation along step edges and why this modulation or the dynamic refacetting leads to a significant change in conductance. Moreover, our recent high-resolution STM study down to 78 K and ARPES down to 70 K could not find any evidence of the $10a_0$ modulation.[18,19]

In this study, we have reinvestigated this surface thoroughly utilizing the conductance measurement with higher surface sensitivity and STM and ARPES with higher resolution in a wider temperature range. As expected from the band structure, the surface conductance shows a metallic behavior down to 140 K in contrast to the previous

measurement.[21,22] Moreover, we could not reproduce the transition at 78 K into a 1D metallic state but, instead, found a significant reduction in the surface conductivity below 140 K. A temperature-dependent STM observation reveals the formation of an out-of-phase ordering of the $2a_0$ interwire modulation for parts of the wires at a consistent temperature range but cannot find any refacetting or a $10a_0$ intrawire modulation. This interwire ordering may suppress the electron transport across the wires to cause the change in the surface conductivity. However, no significant change in the band structure is observed by ARPES, which leaves the origin of the phase transition elusive.

II. EXPERIMENTAL

The experiments were performed in three separated ultrahigh-vacuum systems; a commercial low-temperature STM,[18] an ARPES system with a high-performance electron analyzer (R4000, VG Scienta, Sweden), and a home-build μ4PP system described elsewhere.[5] A μ4PP chip with 20 μm spacing was chosen in the surface-conductivity measurement.[25] The surface reconstruction was checked by LEED in STM and ARPES equipments and reflection high-energy electron diffraction in the μ4PP system. For ARPES measurements, a He discharge lamp was used at the photon energy of 21.2 eV (the He I line). A n-type Si(557) wafer with the bulk resistivity of 10 Ω cm was used, which was cleaned following the established recipe to make a regular step array.[26] The Si(557)$\alpha \times 2$-Pb surface was prepared by depositing $\sim$2 ML of Pb onto a clean Si(557) surface, followed by a mild annealing at 640–650 K.[17–19] The coverage of Pb was calibrated by core-level photoelectron intensities.[17]

III. RESULTS AND DISCUSSION

First, we have measured the electric conductance through surface states with a μ4PP chip as a function of temperature. The measured resistance (R) is shown in Fig. 1(a). The sheet conductance (σ_{meas}) is calculated from R as $\sigma_{meas} = \frac{\ln 2}{\pi R}$ [Fig. 1(b)]. In principle, σ_{meas} contains the surface state, space-charge layer, and bulk contributions all together. However, if there is a strong band bending due to a surface layer on a Si substrate with a proper doping level, then the current within a narrow probe spacing (less than $\sim$100 μm) can be well confined within the surface and space-charge layers.[5,9] For the present system, we estimated, by measuring the Si $2p$ core-level shifts using synchrotron-radiation photoelectron spectroscopy (data not shown),[17] that the bulk valence-band maximum at the surface locates 0.21 eV below the Fermi energy (E_F). This satisfies the proper band-bending condition on the n-type substrate for the current confinement within the surface and space-charge layers in μ4PP measurements. Then, the maximum contribution of the space-charge layer conductance (σ_{sc}) can be calculated easily and reliably by solving the Poisson equation.[5] The calculated space-charge layer conductance is smaller than σ_{meas} by an order of magnitude at RT and decreases further upon cooling (order of 10^{-7} μS at 100 K) as plotted in Fig. 1(b). Therefore, we can
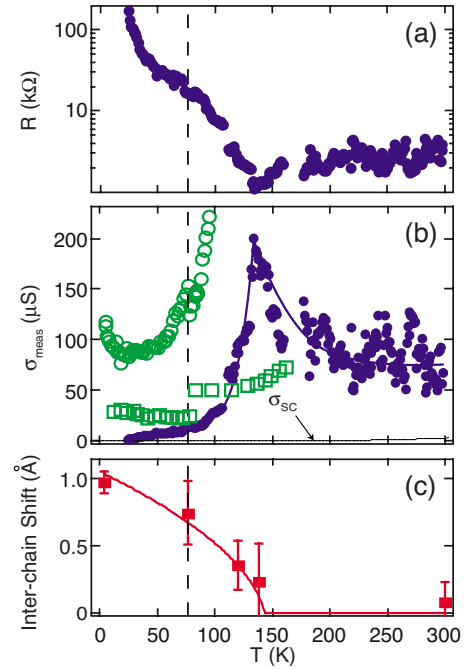

FIG. 1. (Color online) Measured four-point-probe resistance R and the sheet conductance σ_{meas} derived from it for the Si(557)$\alpha \times 2$-Pb surface are plotted as filled circles in (a) and (b), respectively. The open circles and squares [squares from Fig. 3(d) of Ref. 22] in (b) show the corresponding data derived from two previous measurements (Refs. 21 and 22); the geometrical mean of the conductance along and across the wires were taken for comparison. (c) The interwire shift of the protrusions in the STM images shown in Fig. 2. The error bar is the standard deviation in measuring the shift. The lines in (b) and (c) are guides for the eye. T_c of the previously reported conductivity transition is indicated by the vertical broken lines in (a)–(c).

conclude that the space-charge layer contribution is actually negligible and σ_{meas} comes mostly from the surface-state conductance. For the Si(557)$\alpha \times 2$-Pb surface, the surface conductivity at RT is measured to be $\sim$100 μS, which is comparable with those measured for other well-characterized metallic adsorbate layers on Si surfaces.[5,9,12] Supporting further its metallic nature, the conductivity increases upon cooling from 300 K down to 140 K. However, the conductivity starts to decrease abruptly from 140 K. That is, the surface appears to transit into an insulating state at 140 K.

In contrast to the present observation, two previous studies from the same group reported a discrete conductivity change at 78 K.[21,22] Those previous studies used a Van der Paw geometry with a macroscopic 4PP to measure the conductance along and across the wires separately while we used a linearly arranged μ4PP geometry which measures the geometric mean of the conductivity parallel and perpendicular to the wires (step edges).[27] Thus, in order to compare quantitatively, we calculated the geometric mean values of the reported wire-parallel and wire-perpendicular conductivities as shown in Fig. 1(b). One can notice that the two previous studies are not consistent with each other not only in the absolute conductivity values but also in the sign of the relative conductivity change at the transition temperature.

Moreover, these studies do not exhibit any metallic behavior above 78 K in contradiction to the ARPES results.[19,20] Note that we do not see any abrupt conductivity transition at this temperature range but only a change in the slope of the conductivity curve, which is shown more clearly in a logarithmic scale plot of the resistance in Fig. 1(a). Qualitatively speaking, the common feature of the previous studies and the present one is only that there exists an obvious conductivity change at low temperature. We have tried several different samples with similar $\alpha \times 2$ diffraction patterns,[28] which were prepared at slightly different coverages and temperatures. They consistently showed the MIT at 140 K without any sign of an abrupt transition at 78 K, which casts doubt on the possible sample dependence in explaining the apparent discrepancy between previous and present experiments. From the nonmetallic behavior around RT, we speculate that the previous macroscopic 4PP measurements may not have the proper surface sensitivity due to a large probe spacing, which dictates a large portion of the current to pass through space-charge and bulk Si layers.[29,30] It was indeed reported that the conductivity measured at a macroscopic probe spacing ($\gtrsim 1$ mm) is not qualitatively consistent with that probed with a μ4PP on the Si(111)4$\times$1-In surface.[5,31] While we cannot completely rule out the possibility of a phase transition at 78 K within a very limited coverage range, the limited surface sensitivity can also naturally explain why the previous study could not detect the conductivity transition at 140 K.

Second, in order to investigate the structural origin of the drastic conductivity change at 140 K, we have performed temperature-dependent LEED and STM observations. As reported previously,[17,18] the LEED pattern consists of spot arrays in the [7 7 $\overline{10}$] direction and streaky $\times 2$ features between them [see Fig. 2(a)]. Note that this LEED pattern is consistent among previous reports from different research groups. The spot arrays characterize the regular step superstructure (or the periodic nanowire array) with a 15.4 Å ($=4\frac{2}{3}a_0 \cos 30°$) periodicity, which corresponds to four Si unit cells and one step edge. However, as shown in Fig. 2(a), LEED does not show any significant temperature dependence around 140 or 78 K, except for the reduced background intensity at low temperature. As the background intensity is reduced, one can notice weak extra spots as shown in Fig. 2(b). These extra spots might lead the previous study to conclude the formation of a long-period modulation along the wires at low temperature. However, we find little temperature dependence on these spots. Instead, their intensity depends rather sensitively on the Pb coverage (or annealing temperature) as detailed before;[17] its intensity increases at a lower Pb coverage (higher annealing temperature) with the apparent deterioration of the $\alpha \times 2$ LEED features (both spot arrays and streaks) [see Fig. 2(b)]. That is, it is rather clear that these spots come from a different phase from the well-ordered nanowire array as the surface becomes inhomogeneous through the step bunching.[17,18] Indeed, those extra spots, when optimized, can be easily identified as the so-called "linear phase" of the dense Pb overlayer on flat (wider) Si(111) terraces.[17] The hexagonal symmetry of these spots is obvious, appearing around the $\sqrt{3}\times\sqrt{3}$ points, which further corroborates their origin from the 2D Pb overlayer. The recent STM study already confirmed the step bunching
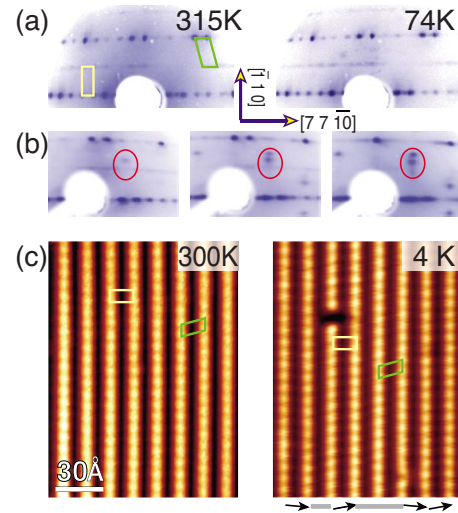

FIG. 2. (Color online) (a) LEED and (c) STM images of the Si(557)-$\alpha \times 2$-Pb surface taken at the temperatures indicated. The STM images were recorded with the tunneling conditions of 0.5 V and 50 pA. Rectangular and oblique $4\frac{2}{3} \times 2$ unit cells are superimposed. The domains of rectangular and oblique unit cells are marked by arrows and gray bars at the bottom of the 4 K STM image in (c). (b) shows the LEED patterns taken at 70 K for the samples with linearly split $\sqrt{3}$-like spots (within the ellipses). These samples were made by annealing at 640 K, 660 K, and 700 K, respectively, following Pb deposition of 2 ML. The incident electron energy was 80 eV for all LEED observations.

at this coverage and temperature range and the formation of a dense Pb 2D overlayer on wider terraces than the nanowire phase.[18]

In real space, STM reveals the well-ordered atomic-scale wire array of the $\alpha \times 2$ phase with a very prominent $2a_0$ modulation in the [$\overline{1}$10] direction at 300 K [Fig. 2(c)]. The same image was observed previously at 78–120 K.[18] Upon decreasing the temperature, we find no change in the STM image down to 4 K at least for the clear intrawire modulation and the interwire spacing as also shown in the figure. This is consistent with the LEED observations and denies more clearly the possibility of a structural transition along the wires.[23] This also denies clearly, at least for the major surface phase composed of nanowires, any change in the interwire spacing or the refaceting transition suggested before based on a LEED result to explain the phase transition at 78 K.[24] That high-resolution LEED study[24] focused on the subtle change in the extra higher order spots, which we assign as due to the minor surface phase on wider terraces. However, the consistent LEED and STM images are also in sharp contrast with the drastic change in the surface conductivity at 140 K discussed above.

This discrepancy provides us the motivation to scrutinize the STM images more carefully. In particular, we focused on the phase of the intrawire $2a_0$ modulation. As we pointed out previously,[18] the lateral coupling of the $2a_0$ modulation between neighboring wires can take both in-phase and out-of-phase configurations. This yields rectangular or oblique 2D unit cells locally [see Fig. 2(c)]. Both units were observed from 300 to 4 K without a noticeable change as shown in
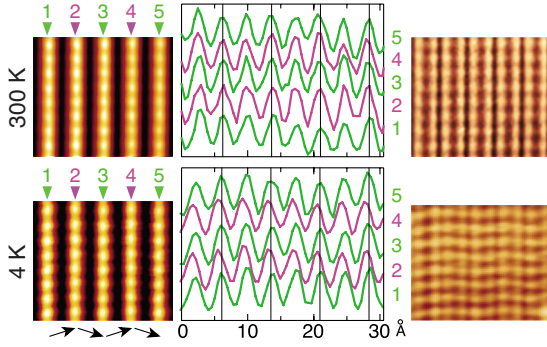
FIG. 3. (Color online) Enlarged STM images (tunneling at 0.5 V and 50 pA) taken at 300 and 4 K (left), their line profiles along the wires (center), and the images after filtering out the Fourier component corresponding to the interwire periodicity (right).

Fig. 2(c). The population ratio of different units did not show a significant change from 300 to 4 K with the rectangular units covering 60–70 % of the surface. However, a careful inspection of the line profiles of the intrawire modulation indicates a subtle interwire ordering [see Fig. 3]. The protrusions shift slightly along the wires between neighboring wires at low temperature to form an alternating interwire order with a doubled periodicity [$2 \times (15.4)$ Å]. This shift was not observed within the wires with the out-of-phase interwire configuration (the oblique unit cells) from RT but only among those with the in-phase configuration (the rectangular unit cells). From the line profile, the shift was measured to be 0.97 ± 0.1 Å. This lateral ordering can be visualized more clearly by taking out the dominant contrast due to the step-terrace structure of the surface. This contrast tends to exaggerate the protrusions along step edges and hide the structure within terraces. The images in the right panel of Fig. 3 was created by Fourier filtering the interwire periodicity ($4\frac{2}{3}a_0 \cos 30°$) from each horizontal line profile of the STM images.[32] The doubled periodicity is clear at 4 K but absent at 300 K.

This interwire ordering has only a very short-length scale as limited by the size of the domains with the rectangular unit cells, eight neighboring wires at maximum ($\lesssim 12$ nm). Thus, it is not detected in the Fourier transform of the STM images (data not shown) and in the LEED patterns [Fig. 2(a)]. However, this ordering is discerned even in the narrowest rectangular domains as indicated by arrows in Fig. 2(c). This subtle shift exhibits a systematic temperature dependence as summarized in Fig. 1(c); the shift is reduced at higher temperatures and disappears above 140 K. This temperature dependence indicates that the interwire shift is related to the conductivity change at 140 K and may be a good order parameter for that phase transition. However, the detailed structural change underlying the shift of the protrusions in the STM image is not clear at all at present.

Since a conductivity change may leave a more pronounced signature in the electronic band structure, we carefully checked the temperature dependence of the surface band structure around 140 K. We have shown in the previous study that the electronic structure of this surface is well described with simple 2D tight-binding bands of Pb in-plane *p* orbitals and the weak periodic potential of the step
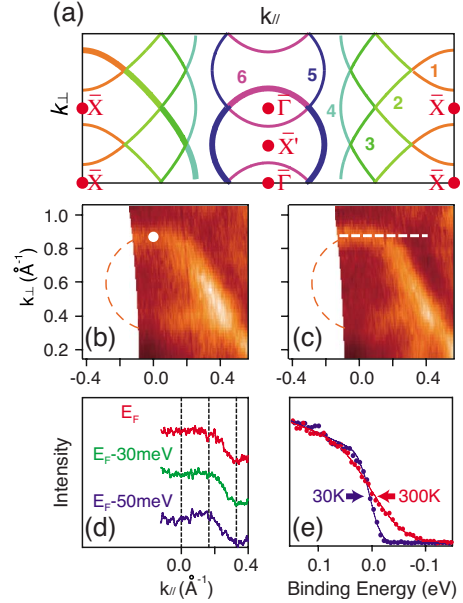

FIG. 4. (Color online) (a) Schematics of Fermi surfaces of Si(557)$\alpha \times 2$-Pb simulated by the tight-binding calculation, which consist of circular $\bar{X}'$ hole pockets and diamond-shaped $\bar{X}$ electron pockets repeated according to the step periodicity (Ref. 19). (b) and (c) show photoelectron-intensity maps around the hole pocket at E_F taken at 300 K and 30 K, respectively, with brighter contrast for higher photoelectron intensity. This hole pocket is traced by broken circles. (d) Photoelectron-intensity profiles (momentum distribution curves) along the dotted line in (c) at the binding energies indicated for the data at 30 K. Dotted lines indicate multiples of $\frac{2\pi}{10a_0}$, that is, the momentum space positions for the $10a_0$ modulation discussed previously. (e) compares photoelectron energy distribution curves at 300 and 30 K taken at the midpoint of $\bar{\Gamma}$ and $\bar{X}'$ indicated by a white dot in (b). Solid lines are fitting curves which convolute Fermi-Dirac distribution function with Gaussian on a linear background.

superlattice.[19] Figure 4(a) shows schematically the 2D FSs, which are based on a diamond-shaped electron pocket around $\bar{X}$ (only a quadrant is shown with a thicker line) and a circular hole pocket around $\bar{X}'$ (three quadrants are shown with a thicker line). They repeat themselves according to the periodicity of the step superlattice and split into the bands denoted as 1–4 and 5 and 6, respectively (the band gaps are not indicated here). The split bands 2–5 form wiggled quasi-1D FSs while 1 and 6 bands, respectively, 2D electron and hole pockets.

While our previous ARPES study could not find any temperature-dependent change in the spectral features,[19] a more recent ARPES study reported that (i) there exists an intensity modulation on the FS due to the long-period ($10a_0$) structure along the wires and (ii) there is a signature of the gap opening, a noticeable reduction in the density of states at E_F, upon cooling.[20] It was not explicitly mentioned whether the long-period modulation of the FS is temperature dependent or not. We, thus, examined the corresponding part of the FS, which is the hole-pocket centered at $\bar{X}'$ within our tight-binding analysis. At first, along the wires, the Fermi contour does not show any significant difference between 300 and 30
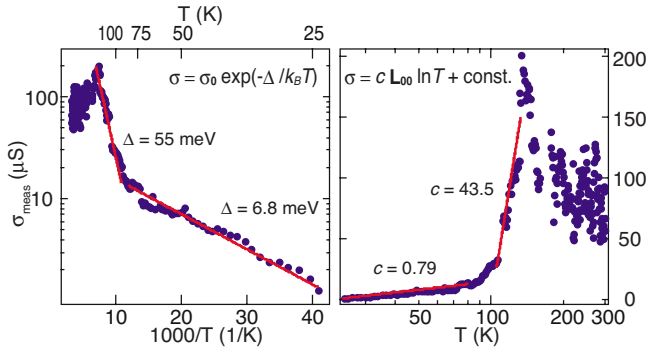
FIG. 5. (Color online) The same data as Fig. 1(a) but plotted logarithmically against the inverse temperature (left) and linearly against the logarithmically scaled temperature (right). The lines in the plots are fitting results by $\sigma = \sigma_0 \exp(-\Delta/k_B T)$ (left) and $\sigma = c L_{00} \ln T + \text{const.}$ (right), where $L_{00} = 12.3 \ \mu S$.

K [Figs. 4(b) and 4(c)]. Furthermore, the detailed momentum distribution curves at and below E_F exhibit no temperature dependence and no sign of a modulation due to a long-period superstructure [Fig. 4(d)]. All around this hole pocket, the energy distribution curve (EDC) keeps consistent spectral weight at E_F between the two temperatures, ruling out the possibility of a significant energy gap [Fig. 4(e)]. By a careful fitting of the EDCs, we estimate that any possible gap should be smaller than $\sim 5 - 10$ meV at 30 K. Therefore, this result, performed with a higher energy and momentum resolution than the previous studies, denies the possibility of the formation of the superstructure along the wires in accord with STM and LEED observations. It also indicates that the effect of the subtle interwire order observed has little effect on the overall band structure. This may be due to the fact that the coherence length of the extra interwire order at low temperature is too short to produce any change in the band structure. In summary, the detailed ARPES study does not provide any clue to understand the drastic change in the surface conductivity (or the conductivity transition reported at 78 K).

Note that the present conductance transition is distinct from the MITs known for other metallic systems on Si surfaces and looks apparently more complex than them. The transitions in the 1D metallic systems of Si(111)4×1-In and Si(553)-Au accompany the complete gap opening and strong lattice (charge) modulations.[7,8] These systems exhibit the strongly anisotropic conductance, which drops drastically by more than three orders of magnitude within several 10 K below the transition temperature.[5,9] This is not the case for the present surface which keeps the metallic band structure even below T_c. Moreover, the Arrhenius plot of the conductance is apparently not a single linear function below T_c but breaks into two lines; the steep one with an activation energy of $\Delta = 55$ meV above ~ 100 K and the gentle one with $\Delta = 6.8$ meV below ~ 80 K (Fig. 5). That is, the transition cannot be explained by a single gap-opening transition. Although the lattice modulation is also noticed in the present system, it is thought to be fairly weak. It is worth noting that the present transition accompanies not a global but a local structural change; the surface is a mixture of two domains with small domain sizes in the interwire direction and the structural change occurs only within one domain. It may be

possible that this local change can disturb the conduction channel across the wires through the enhanced scattering to lead to the observed behavior in surface transport measurements. The possible band-structure change may be blurred out due to the very limited domain size and the possible band gap involved is as small as 7–55 meV.

On the other hand, a different type of MIT was found on the 2D metallic system of Si(111)$\sqrt{3} \times \sqrt{3}$-Ag with a tiny amount of defects or adatoms.[12,13] This surface does not exhibit any change in its band structure through the MIT in conductance as in the present system. The driving force of the MIT was argued in terms of the weak or strong localization caused by the random potentials provided by scatterers and enhanced by the electron standing waves.[12] We thus checked the possibility of a localization transition for the present case. In the right panel of Fig. 5, σ_{meas} is plotted against logarithmically scaled temperature. Since the surface has a largely 2D electronic structure, we fitted σ_{meas} below T_c with the theoretical curve of the 2D weak localization model, $\sigma = c L_{00} \ln T + \text{const.}$, where $L_{00} = 12.3 \ \mu S$, the quantum conductance divided by 2π. The parameter c, which is related to the exponent of T for the inverse phase relaxation time of electrons, is reported to be 0.75 in a thin film[33] and 0.71–0.90 in inversion layers of semiconductors.[34] Comparable values were also obtained for the localization cases in other surface systems.[13,35] The fitting is successful for the present system below ~ 80 K with a reasonable value of $c = 0.79$, but fails above ~ 100 K with an unnaturally large c of 43.5. Thus, although the electrons can be weakly localized in the low-temperature region ($T \lesssim 80$ K), the transition at 140 K cannot be explained in this way. The previously found transition at 78 K might be related to the onset of the weak localization. Note that the other theories based on the weak localization in 1D ($\sigma \propto T^{-1/2}$) or the variable-range hopping case in 2D ($\sigma \propto \exp[-(\Delta/k_B T)^{1/3}]$) or 1D ($\sigma \propto \exp[-(\Delta/k_B T)^{1/2}]$) cannot fit the obtained conductance change at all. The above comparison of the characteristics of the present phase transition with other systems manifests the uniqueness of the present one but the transition mechanism itself remains elusive.

IV. CONCLUSIONS

The temperature dependence in the electron transport and atomic and electronic band structures of the Si(557)$\alpha \times 2$-Pb surface, a regular Pb-nanowire array on a stepped Si surface was reinvestigated by μ4PP conductivity measurements, STM, LEED, and ARPES. The surface exhibits a substantial reduction in its electric conductance at 140 K in contrast to the previous study reporting a rather minor change at 78 K. We could not find any change in the structure along the wires claimed previously. Instead, STM shows that this transition is accompanied by the subtle period-doubling interwire ordering which occurs on part of the surface. While we cannot completely rule out the possibility of a phase transition at 78 K within a very limited coverage range, this metal-

insulator-type transition is found to prevail for most of Pb coverages with a good $\alpha \times 2$ ordering. However, the overall band structure does not change within the experimental resolution, which denies the partial gap opening raised to explain the conductivity change at 78 K. The present observation may indicate a drastic change in the electron-scattering process across the wires through the interchain-order formation while the structural details of the interwire order and the microscopic mechanism of the conductivity change remain elusive.

*yeom@postech.ac.kr

[1] N. F. Mott, *Metal-Insulator Transitions*, 2nd ed. (Taylor & Francis, New York, 1990).

[2] J. G. Bednorz and K. A. Müller, Z. Phys. B: Condens. Matter **64**, 189 (1986).

[3] I. J. Lee, M. J. Naughton, G. M. Danner, and P. M. Chaikin, Phys. Rev. Lett. **78**, 3555 (1997).

[4] I. Barke, R. Bennewitz, J. N. Crain, S. C. Erwin, A. Kirakosian, J. L. McChesney, and F. J. Himpsel, Solid State Commun. **142**, 617 (2007).

[5] T. Tanikawa, I. Matsuda, T. Kanagawa, and S. Hasegawa, Phys. Rev. Lett. **93**, 016801 (2004).

[6] H. W. Yeom, S. Takeda, E. Rotenberg, I. Matsuda, K. Horikoshi, J. Schaefer, C. M. Lee, S. D. Kevan, T. Ohta, T. Nagao, and S. Hasegawa, Phys. Rev. Lett. **82**, 4898 (1999).

[7] J. R. Ahn, J. H. Byun, H. Koh, E. Rotenberg, S. D. Kevan, and H. W. Yeom, Phys. Rev. Lett. **93**, 106401 (2004).

[8] J. R. Ahn, P. G. Kang, K. D. Ryang, and H. W. Yeom, Phys. Rev. Lett. **95**, 196402 (2005).

[9] H. Okino, I. Matsuda, S. Yamazaki, R. Hobara, and S. Hasegawa, Phys. Rev. B **76**, 035424 (2007).

[10] T. Aruga, Surf. Sci. Rep. **61**, 283 (2006).

[11] R. G. Moore, J. Zhang, V. B. Nascimento, R. Jin, J. Guo, G. T. Wang, Z. Fang, D. Mandrus, and E. W. Plummer, Science **318**, 615 (2007).

[12] I. Matsuda, C. Liu, T. Hirahara, M. Ueno, T. Tanikawa, T. Kanagawa, R. Hobara, S. Yamazaki, S. Hasegawa, and K. Kobayashi, Phys. Rev. Lett. **99**, 146805 (2007).

[13] C. Liu, I. Matsuda, S. Yoshimoto, T. Kanagawa, and S. Hasegawa, Phys. Rev. B **78**, 035326 (2008).

[14] H. Morikawa, I. Matsuda, and S. Hasegawa, Phys. Rev. B **70**, 085412 (2004).

[15] A. van Houselt, T. Gnielka, J. M. J. Aan de Brugh, N. Oncel, D. Kockmann, R. Heid, K. Bohnen, B. Poelsema, and H. J. W. Zandvliet, Surf. Sci. **602**, 1731 (2008).

[16] J. N. Crain, A. Kirakosian, K. N. Altmann, C. Bromberger, S. C. Erwin, J. L. McChesney, J.-L. Lin, and F. J. Himpsel, Phys. Rev. Lett. **90**, 176805 (2003).

[17] K. S. Kim, W. H. Choi, and H. W. Yeom, Phys. Rev. B **75**, 195324 (2007).

[18] H. Morikawa, K. S. Kim, D. Y. Jung, and H. W. Yeom, Phys. Rev. B **76**, 165406 (2007).

[19] K. S. Kim, H. Morikawa, W. H. Choi, and H. W. Yeom, Phys. Rev. Lett. **99**, 196804 (2007).

[20] C. Tegenkamp, T. Ohta, J. L. McChesney, H. Dil, E. Rotenberg, H. Pfnür, and K. Horn, Phys. Rev. Lett. **100**, 076802 (2008).

[21] C. Tegenkamp, Z. Kallassy, H. Pfnür, H.-L. Günter, V. Zielasek, and M. Henzler, Phys. Rev. Lett. **95**, 176804 (2005).

[22] C. Tegenkamp, Z. Kallassy, H.-L. Günter, V. Zielasek, and H. Pfnür, Eur. Phys. J. B **43**, 557 (2005).

[23] M. Czubanowski, A. Schuster, S. Akbari, H. Pfnür, and C. Tegenkamp, New J. Phys. **9**, 338 (2007).

[24] M. Czubanowski, A. Schuster, H. Pfnür, and C. Tegenkamp, Phys. Rev. B **77**, 174108 (2008). This paper claims that one Si row is added to every sixth (111) terrace on the (223) facet above 78 K, changing the average orientation of the facet to (17 17 25). However, in order to form the (17 17 25) plane, one Si row should be added to every third (111) terrace.

[25] http://www.capres.com/

[26] A. Kirakosian, R. Bennewitz, J. N. Crain, Th. Fauster, J.-L. Lin, D. Y. Petrovykh, and F. J. Himpsel, Appl. Phys. Lett. **79**, 1608 (2001).

[27] J. D. Wasscher, Philips Res. Rep. **16**, 301 (1961).

[28] See supplementary material at http://link.aps.org/supplemental/10.1103/PhysRevB.82.045423 for the corresponding reflection high-energy electron-diffraction pattern.

[29] S. Hasegawa, X. Tong, S. Takeda, N. Sato, and, T. Nagao, Prog. Surf. Sci. **60**, 89 (1999).

[30] Ph. Hofmann and J. W. Wells, J. Phys.: Condens. Matter **21**, 013003 (2009).

[31] T. Uchihashi and U. Ramsperger, Appl. Phys. Lett. **80**, 4169 (2002).

[32] GWYDDION package, http://gwyddion.net/

[33] R. S. Markiewicz and L. A. Harris, Phys. Rev. Lett. **46**, 1149 (1981).

[34] B. J. F. Lin, M. A. Paalanen, A. C. Gossard, and D. C. Tsui, Phys. Rev. B **29**, 927 (1984).

[35] S. Yamazaki, I. Matsuda, H. Okino, H. Morikawa, and S. Hasegawa, Phys. Rev. B **79**, 085317 (2009).